

Communication

Improving the Luminescence and Stability of Carbon-Centered Radicals by Kinetic Isotope Effect

Zhichao Ma ^{1,†}, Lintao Zhang ^{1,†}, Zhiyuan Cui ² and Xin Ai ^{1,*} 

¹ School of Materials Science and Engineering, Collaborative Innovation Center of Information Technology, Collaborative Innovation Center of Marine Science and Technology, Hainan University, No 58, Renmin Avenue, Haikou 570228, China; 20080500210020@hainanu.edu.cn (Z.M.); zhanglintao@hainanu.edu.cn (L.Z.)

² State Key Laboratory of Supramolecular Structure and Materials, College of Chemistry, Jilin University, No. 2699, Qianjin Avenue, Changchun 130012, China; zycui2021@163.com

* Correspondence: aixin133@hainanu.edu.cn

† These authors contributed equally to this work.

Abstract: The kinetic isotope effect (KIE) is beneficial to improve the performance of luminescent molecules and relevant light-emitting diodes. In this work, the influences of deuteration on the photophysical property and stability of luminescent radicals are investigated for the first time. Four deuterated radicals based on biphenylmethyl, triphenylmethyl, and deuterated carbazole were synthesized and sufficiently characterized. The deuterated radicals exhibited excellent redox stability, as well as improved thermal and photostability. The appropriate deuteration of relevant C-H bonds would effectively suppress the non-radiative process, resulting in the increase in photoluminescence quantum efficiency (PLQE). This research has demonstrated that the introduction of deuterium atoms could be an effective pathway to develop high-performance luminescent radicals.

Keywords: organic luminescent radical; biphenylmethyl; triphenylmethyl; deuteration; kinetic isotope effect



Citation: Ma, Z.; Zhang, L.; Cui, Z.; Ai, X. Improving the Luminescence and Stability of Carbon-Centered Radicals by Kinetic Isotope Effect. *Molecules* **2023**, *28*, 4805. <https://doi.org/10.3390/molecules28124805>

Academic Editor: Jiaren Du

Received: 25 May 2023

Revised: 13 June 2023

Accepted: 14 June 2023

Published: 16 June 2023



Copyright: © 2023 by the authors. Licensee MDPI, Basel, Switzerland. This article is an open access article distributed under the terms and conditions of the Creative Commons Attribution (CC BY) license (<https://creativecommons.org/licenses/by/4.0/>).

1. Introduction

Organic radicals with unpaired electrons exhibit great application prospects for their unique optical, electrical, and magnetic properties [1–10]. Especially, through the doublet emission process, the theoretical upper limit of the internal quantum efficiency for radical-based light-emitting devices can reach 100% [11,12]. In order to improve the properties of luminescent radicals, several molecular design strategies were proposed. Guo et al. designed a few triphenylmethyl derivatives with different electron-rich groups, the electron structure of which did not follow the Aufbau principle, which exhibited higher photostability and photoluminescence quantum efficiency (PLQE) [13]. Alim et al. proposed the introduction of specific groups to construct non-alternant hydrocarbon which was beneficial to improve PLQE [14]. Mattiello et al. improved the photostability of PyBTM derivatives with the introduction of four phenyl groups, which improved even further when extra methoxy groups were added [15]. With terminal benzene rings on carbazole, Matsuda et al. improved the photostability of TTM-1Cz radicals efficiently [16]. Moreover, many studies have explored the effects of different substituent groups on the properties of luminescent bi- or triphenylmethyl radicals [17–22].

In addition to incorporating different substituted groups, the substitution of isotopes on relevant C-H bonds could also influence the properties of luminescent molecules, especially PLQE and stability [23,24]. Although the steric and electronic configurations are barely influenced, isotopic replacement of the protium atom (H) by the deuterium atom (D) would enormously change the bond stretch bands and decrease the energy of vibration modes, namely the kinetic isotope effect (KIE) of H/D substitution. Usually, after being substituted by D, the non-radiative transitions of molecules would be suppressed

and the rates of relevant C-H(D) bond breaking would be decreased, resulting in higher PLQE and better stability under heated or irradiated conditions, even in working light-emitting diodes. Thus, the deuteration of relevant chemical bonds has become an effective way to develop high-performance luminescent materials, as well as light-emitting diodes based on closed-shell molecules with fluorescence, phosphorescence, or thermally activated delayed fluorescence (TADF) [25–29]. However, up until now, the KIE on properties of open-shell luminescent radicals has not been reported. Hence, in this work, molecules based on different luminescent radical systems with different numbers of deuterated carbazole groups were synthesized to investigate the KIE on properties of open-shell radicals, especially PLQE and stability.

2. Results and Discussion

2.1. Synthesis and Structure Characterization

Based on two typical luminescent radical systems, biphenylmethyl radical and triphenylmethyl radical, we synthesized four luminescent radicals with one or two deuterated carbazole groups, (N-deuterocarbazolyl)bis(2,4,6-trichlorophenyl)methyl radical (**BTM-1DCz**), (N-deuterocarbazolyl)[4-(N-deuterocarbazolyl)-2,6-dichlorophenyl] (2,4,6-trichlorophenyl)methyl radical (**BTM-2DCz**), [4-(N-deuterocarbazolyl)-2,6-dichlorophenyl]bis(2,4,6-trichlorophenyl)methyl radical (**TTM-1DCz**), as well as bis[4-(N-deuterocarbazole)-2,6-dichlorophenyl](2,4,6-trichlorophenyl)methyl radical (**TTM-2DCz**) (Figure 1). Their non-deuterated molecules (**BTM-1Cz**, **BTM-2Cz**, **TTM-1Cz** and **TTM-2Cz**) and classical radical **TTM** were also synthesized for comparison. The synthetic route followed the methods reported in the literature by using commercial materials [30,31]. There are few C-H bonds either in the biphenylmethyl or triphenylmethyl skeleton, which means the majority of C-H bonds were deuterated in the four target radicals. Since radicals are mostly silent in NMR measurements for their spin characteristics, the molecular structure and composition of target radicals were mainly confirmed by characterization of high-resolution mass spectrometer (HRMS) (Figure S2), FTIR, and elemental analysis (EA). Unlike the reported non-deuterated molecules, similar absorption peaks around 2280 cm^{-1} resulting from the aromatic C-D bond stretch, were found in the FTIR spectra of these four radicals (Figure S3). The existence of unpaired electrons in radicals was confirmed by electron paramagnetic resonance (EPR) measurements (Figure S4), the g values around 2.0040 demonstrate the feature of single free electrons.

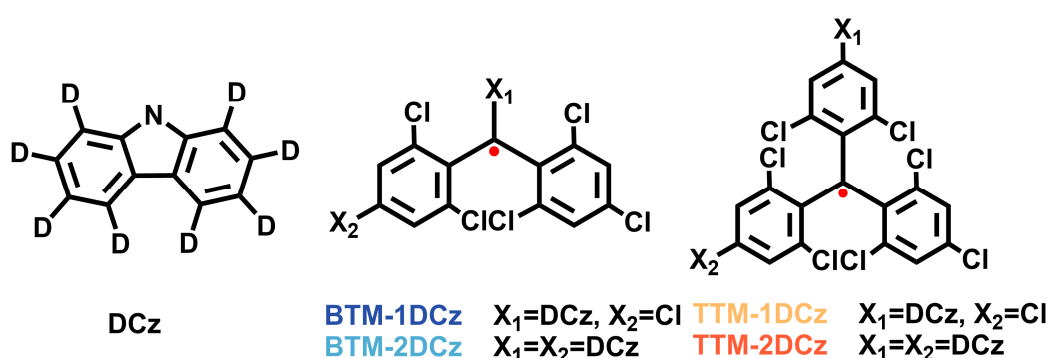


Figure 1. Molecular structures of **BTM-1DCz**, **BTM-2DCz**, **TTM-1DCz**, **TTM-2DCz**, and deuterated carbazole (**DCz**).

2.2. Photophysical Properties

The ultraviolet-visible (UV-Vis) absorption spectra of four radicals were measured in cyclohexane solvent (Figure 2). Most of them show three typical absorption bands. The strong absorption bands, peaking at 285 nm for **BTM-1DCz** and **BTM-2DCz**, and 290 nm for **TTM-1DCz** and **TTM-2DCz**, come from carbazole. The medium absorption bands, peaking at 375 and 387 nm for **TTM** series and **BTM-1DCz**, and 369 and 403 nm for **BTM-**

2DCz, are the characteristic absorption from carbon-centered radicals. Additionally, the weak absorption bands of four radicals, peaking from 450 to 700 nm which are not identical, mainly come from the intramolecular charge–transfer states compared with previous research [30,31]. Compared to the non-deuterated molecules, there is no significant change for the UV-Vis absorption spectra since there was no obvious transformation for both steric and electronic configurations between deuterated and non-deuterated molecules. In addition, **BTM-2DCz**, the only one whose non-deuterated molecule has not been reported before, shows some differences in absorption spectrum. There is an obvious absorption band peaking at 470 nm different from **BTM-1DCz**, and slight absorption enhancement around 600 nm. That is because two carbazole groups in **BTM-2DCz** are located at different sites. One is similar to the site in **BTM-1DCz**, and the other is similar to the site in **TTM-1DCz**. Thus, there would be two possible types of intramolecular charge–transfer in **BTM-2DCz**, resulting in the changes of long-wavelength absorption compared to the spectra of **BTM-1DCz** and **TTM-1DCz**. With increasing carbazole groups, the absorption of carbazole around 280 nm clearly increases. At the same time, the ratios of absorption from charge–transfer state at long wavelengths to absorption from carbon-center radicals around 380 nm are also increased, which indicates more characteristics of the charge–transfer state in more carbazole-substituted radicals. Absorption spectra in different solvents with different polarity were also measured (Figure S5), and no obvious change could be found.

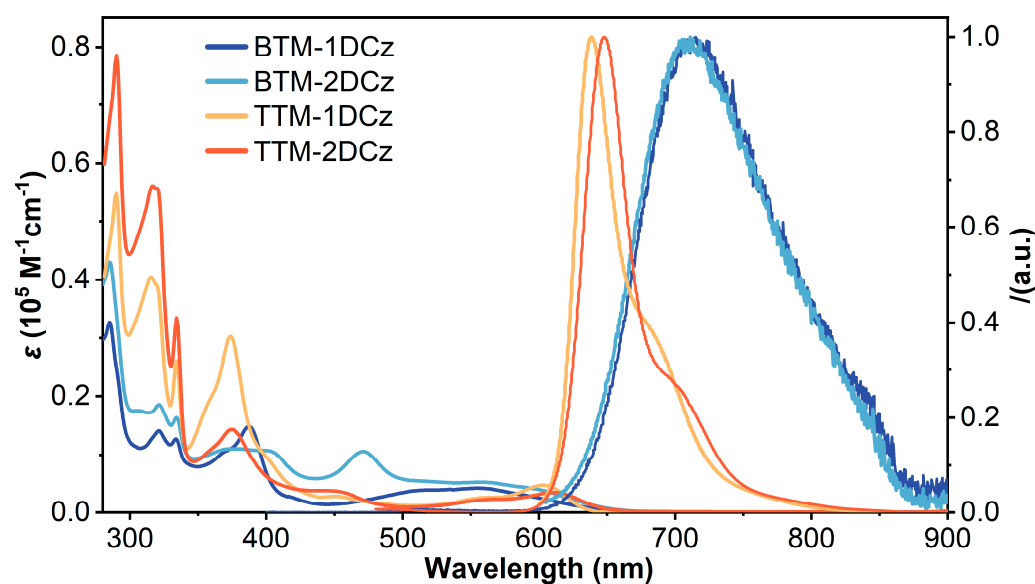


Figure 2. UV-Vis absorption and normalized PL spectra of four deuterated radicals in cyclohexane solvent (1×10^{-5} M).

Photoluminescence (PL) spectra of deuterated radicals were measured in cyclohexane solvent (Figure 2). **BTM-1DCz** and **BTM-2DCz** exhibit weak deep-red emission peaking at 711 and 706 nm, respectively. The absolute PLQE values measured by integrating sphere are 3.0% for **BTM-1DCz** and 3.6% for **BTM-2DCz**. **TTM-1DCz** and **TTM-2DCz** exhibit bright red emission peaking at 638 and 647 nm with considerable absolute PLQE values of 78.4 and 56.7%, respectively. Similar to absorption spectra, besides slight blue-shift, there is no obvious change in PL spectra of all deuterated radicals compared to non-deuterated molecules (Figure 2). It is noteworthy that the PLQE values of **BTM-1DCz** and **TTM-1DCz** in cyclohexane are almost 1.5 times as high as the relevant non-deuterated molecules reported in the literature [30,31].

To better explore the KIE on the luminescent properties of deuterated radicals, the transient PL decays of four radicals in cyclohexane were measured, as well as the unreported relevant photophysical parameters of **BTM-2Cz**. According to the measurements, radiative and non-radiative transition rates of luminescent radicals, k_r and k_{nr} , were calcu-

lated, respectively. All the relevant photophysical parameters are summarized in Table 1. From the results, the k_{nr} values of **BTM-1DCz** and **BTM-2DCz** decrease significantly from 245.0×10^6 and 241.8×10^6 to 215.5×10^6 and $214.2 \times 10^6 \text{ s}^{-1}$ compared to the relevant non-deuterated molecules. A similar reduction could also be found for the k_{nr} values of **TTM-1DCz** and **TTM-2DCz**. However, the k_r values of these four deuterated radicals show few variations. These photophysical results indicate that the deuteration of luminescent radicals does not influence the pathway and probability of radiative transitions, but significantly influences the non-radiative transitions. Because of the KIE from deuterium atoms, the non-radiative transitions of radicals were suppressed effectively, resulting in higher PLQE. The longer fluorescence lifetimes of deuterated radicals also indicate the effective suppression of bond breaking, that is to say the excited states of deuterated radicals become more stable. No matter which radical systems are used, bi- or triphenylmethyl radicals, more deuterated carbazole groups do not yield stronger suppression, so the PLQE values of **BTM-2DCz** and **TTM-2DCz** show little increases. Meanwhile, if the ratios of k_{nr} to k_r of luminescent radicals are as larger as biphenylmethyl radical systems, the influences on PLQE from the KIE of deuteration would be weak. For luminescent radicals with more balanced k_{nr} and k_r , appropriate deuteration could significantly improve PLQE values.

Table 1. Photophysical parameters of deuterated and non-deuterated radicals.

	λ_{Em} (nm)	PLQE (%)	τ (ns)	k_r (10^6 s^{-1})	k_{nr} (10^6 s^{-1})
BTM-1DCz	711	3.0	4.5	6.7	215.5
BTM-1Cz ^a	712	2.0 ^b	4.0 ^b	5.0 ^b	245.0 ^b
BTM-2DCz	706	3.6	4.5	8.0	214.2
BTM-2Cz	707	3.3	4.0	8.2	241.8
TTM-1DCz	638	78.4	41.4	19.0	5.0
TTM-1Cz	640	53.0 ^c	25.3 ^c	21.0	19.0
TTM-2DCz	647	56.7	33.3	17.0	13.0
TTM-2Cz	650	54.0 ^c	28.0 ^c	19.0	17.0

^a. **BTM-1Cz**, namely **CzBTM** in ref. [30]; ^b. Cited from ref. [30]; ^c. Cited from ref. [31].

2.3. Electrochemical Properties

Cyclic voltammetry (CV) analysis was performed to study the redox characteristics of deuterated radicals. Similar to non-deuterated radicals (Figure S7), all of the results mainly show two pairs of reversible redox peaks (Figure 3), indicating the reversible redox properties of deuterated radicals. The initial reduction potentials of **BTM-1DCz** and **BTM-2DCz** are -0.89 and -0.92 V, and the initial oxidation potentials are -0.02 and -0.08 V, respectively. For **TTM-1DCz** and **TTM-2DCz**, the initial reduction potentials are -0.93 and -0.97 V, and the initial oxidation potentials are 0.49 and 0.38 V. With more deuterated carbazole groups, the conjugation of molecules would be increased, resulting in lower redox potentials. Utilizing the measurements of redox potentials, the energy levels of singly occupied molecular orbital (SOMO) and singly unoccupied molecular orbital (SUMO) were calculated. In the order of **BTM-1DCz**, **BTM-2DCz**, **TTM-1DCz**, **TTM-2DCz**, the SOMO energy levels are -4.71 , -4.65 , -5.22 , -5.21 V, and the SUMO energy levels are -3.84 , -3.81 , -3.80 , -3.76 V. All the values show little differences compared to non-deuterated radicals (Table S1).

To test the redox stability of deuterated radicals, continuous multicycle (20 cycles) CV measurements were performed. From the relevant CV curves (Figure S8), neither the potentials nor the signal intensities of the redox peaks changed clearly. These results demonstrate that the unpaired electron features and molecular structures would not change after continuous multicycle CV scan, indicating the excellent redox stability of deuterated radicals.

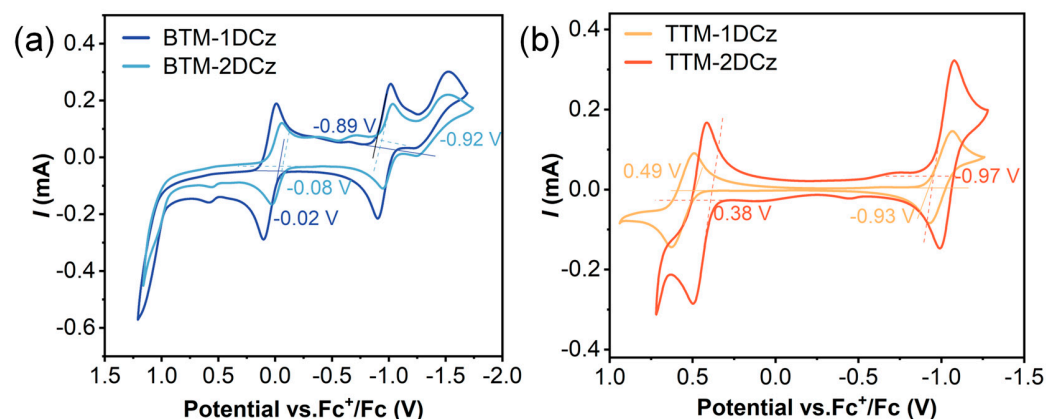


Figure 3. Cyclic voltammetry (CV) curves of (a) **BTM-1DCz** and **BTM-2DCz**; (b) **TTM-1DCz** and **TTM-2DCz**. Ferrocene cation/ferrocene (Fc^+/Fc) couples were used as reference.

2.4. Theoretical Calculations

Density functional theory (DFT) calculations (B3LYP/6-31G(d,p)) and time-dependent density functional theory (TD-DFT) calculations (CAM-B3LYP/6-31 G(d,p)) were performed to further investigate the electronic structures and transitions of deuterated radicals. Frequency calculations were carried out to ensure that all the optimized structures were minima on the potential energy surface. Figure 4 shows the optimized ground state structures and frontier orbitals of deuterated radicals. Compared to non-deuterated radicals, the calculation results did not clearly change due to the negligible influence on electronic structures from deuteration. The frontier energy levels calculated from DFT are almost the same as the SOMO and SUMO energy levels calculated from the CV measurements (Table S2). From the results of optimized TD-DFT calculations, the emission process of radicals, namely the transitions between the lowest doublet excited states (D_1) and the doublet ground states (D_0), are mainly the transitions between SUMO and β -HOMO. All the electron cloud changes of these transitions are from the donors, carbazole parts to the radical centers, demonstrating the charge–transfer feature of luminescence from these radicals. The relevant calculation results of excited states are summarized in Table S3.

2.5. Thermal and Photostability

Stability is a vital property in influencing the applications of luminescent radicals in most fields. Besides the redox stability discussed above, the thermal stability was also evaluated using thermogravimetric analysis (TGA). The results show that the thermal decomposition temperatures of the deuterated radicals are raised in different degrees due to the KIE from deuteration (Figure S9). In particular, the thermal decomposition temperatures of **BTM-1DCz** and **TTM-2DCz** are about 20 °C higher than non-deuterated radicals.

Another important stability that needs to be considered for luminescent radicals is photostability. The decays of fluorescence intensity from deuterated radicals were recorded under continuous irradiation from xenon lamp and contrasted with non-deuterated radicals and **TTM** radicals. The data of these decays were fitted, and the half-life was calculated (Figure 5). The half-life values of the deuterated radicals were 5.39×10^3 (**BTM-1DCz**), 1.32×10^4 (**BTM-2DCz**), 8.57×10^3 (**TTM-1DCz**), and 1.54×10^4 s (**TTM-2DCz**), respectively, indicating excellent photostability. Even compared with non-deuterated radicals, the photostability increases around 2 to 10 times (Figure S10). These results indicate that the photostability of luminescent radicals could be notably increased by deuteration, namely the excited states of luminescent radicals would be more stable due to the KIE, which is beneficial for applications.

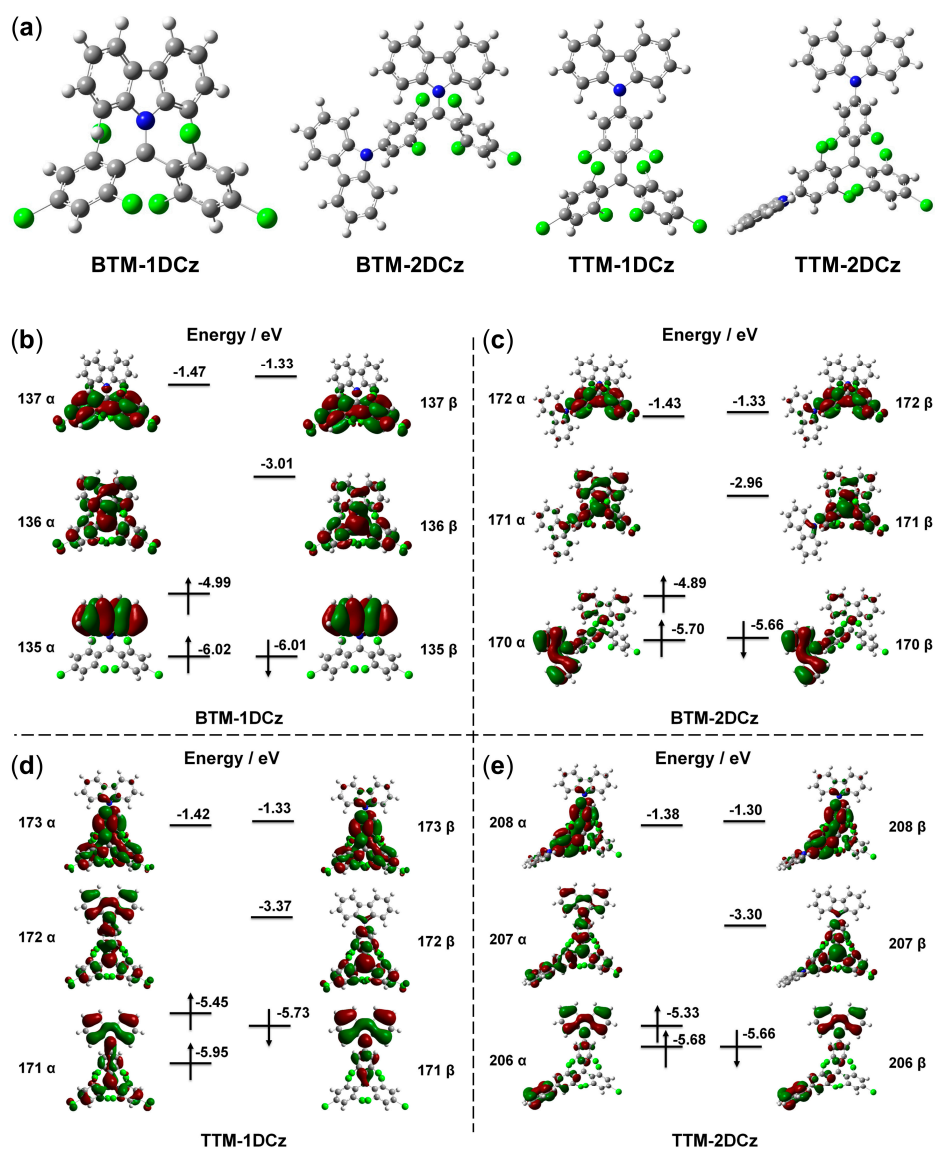


Figure 4. (a) Optimized molecular structures of deuterated radicals. The frontier orbitals of deuterated radicals (b) BTM-1DCz, (c) BTM-2DCz, (d) TTM-1DCz, and (e) TTM-2DCz.

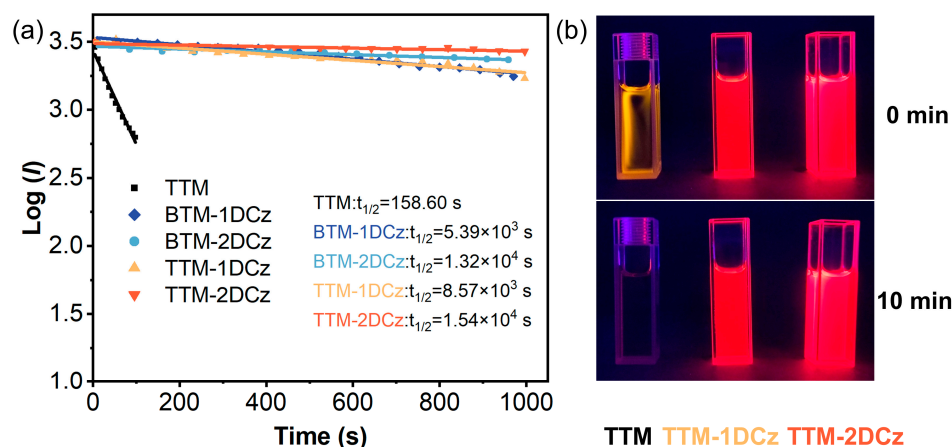


Figure 5. (a) Photostability of deuterated radicals in cyclohexane solution. (b) Photograph of comparison of photostability under irradiation with 365 nm handheld UV lamp.

3. Materials and Methods

All chemical reagents and starting materials used in this work were purchased from ERNEGI and Xilong Science Co., Ltd. (Shanghai, China) without further purification. The synthetic routes of target radicals followed the previous literature and can be found in Supplementary Materials Figure S1.

HRMS were recorded on a Shimadzu LCMS-IT-TOF. Infrared spectra were recorded on a Bruker Tensor 27 spectrometer. Elemental analysis data were recorded on an Elementar Vario microcube spectrometer. EPR data were measured using a Bruker Instruments A320 spectrometer with 10^{-5} M concentration in cyclohexane at room temperature. The UV-Vis spectra in various solvents were measured with a Shimadzu UV-1900i UV-Vis spectrometer. The PL spectra in cyclohexane were measured with a Shimadzu RF-6000 spectrometer. The transient PL decays were recorded using an Edinburgh FLS1000 spectrometer, and the absolute PLQEs were recorded on the same instrument using the integrating sphere method. DFT and TD-DFT calculations were performed on Gaussian16 commercial software (Revision C.02) [32]. Thermal stability measurements were performed on a TA INSTRUMENTS Q600 TGA analyzer under air and a ramp rate of $10\text{ }^{\circ}\text{C}\cdot\text{min}^{-1}$. The CV measurements were performed using a CH Instruments CHI660E electrochemical analyzer with a glassy carbon electrode as the working electrode, a platinum wire as the counter electrode, and Ag/AgCl as the reference electrode. Redox couple ferrocenium/ferrocene was used as an internal standard. The photostability was also recorded on RF-6000 under continuous irradiation from a xenon lamp.

3.1. Synthesis of BTM-1DCz and BTM-2DCz

Compound **BTM-1DCz** and **BTM-2DCz** were prepared following the literature procedure (Figure S1) [30]. Purple-black solid **BTM-1DCz** and dark green solid **BTM-2DCz** were simultaneously obtained from the final step with yields of 22 and 18%, respectively.

BTM-1DCz. LC-HRMS (m/z), calculated for $\text{C}_{25}\text{H}_4\text{D}_8\text{Cl}_6\text{N}^{\bullet}$ $[\text{M}]^+$: 545.9574. Found: 545.9514. **Elemental analysis**, calculated for $\text{C}_{25}\text{H}_4\text{D}_8\text{Cl}_6\text{N}^{\bullet}$ (%): C, 54.88; H, 3.68; N, 2.56. Found (%): C, 54.84; H, 3.65; N, 2.58.

BTM-2DCz. LC-HRMS (m/z), calculated for $\text{C}_{37}\text{H}_4\text{D}_{16}\text{Cl}_5\text{N}_2^{\bullet}$ $[\text{M}]^+$: 685.1044. Found: 685.1006. **Elemental analysis**, calculated for $\text{C}_{37}\text{H}_4\text{D}_{16}\text{Cl}_5\text{N}_2^{\bullet}$ (%): C, 64.79; H, 5.29; N, 4.08. Found (%): C, 64.77; H, 5.26; N, 4.11.

3.2. Synthesis of TTM-1DCz and TTM-2DCz

Compound **TTM-1DCz** and **TTM-2DCz** were prepared following the procedure in the literature (Figure S2) [31]. Reddish-brown solid **TTM-1DCz** was obtained with 71% yield of relevant step, and dark green solid **TTM-2DCz** was obtained with 83% yield of relevant step.

TTM-1DCz. LC-HRMS (m/z), calculated for $\text{C}_{31}\text{H}_6\text{D}_8\text{Cl}_8\text{N}^{\bullet}$ $[\text{M}]^+$: 691.9078. Found: 691.9042. **Elemental analysis**, calculated for $\text{C}_{31}\text{H}_6\text{D}_8\text{Cl}_8\text{N}^{\bullet}$ (%): C, 53.80; H, 3.20; N, 2.02. Found (%): C, 53.78; H, 3.23; N, 2.02.

TTM-2DCz. LC-HRMS (m/z), calculated for $\text{C}_{43}\text{H}_6\text{D}_{16}\text{Cl}_7\text{N}_2^{\bullet}$ $[\text{M}]^+$: 829.0517. Found: 829.0498. **Elemental analysis**, calculated for $\text{C}_{43}\text{H}_6\text{D}_{16}\text{Cl}_7\text{N}_2^{\bullet}$ (%): C, 62.16; H, 4.61; N, 3.37. Found (%): C, 62.17; H, 4.59; N, 3.39.

4. Conclusions

In summary, four deuterated luminescent radicals were synthesized to explore the KIE on luminescent radicals. The non-radiative process could be effectively suppressed by deuteration, which is beneficial to the PLQE of luminescent radicals. In particular, the PLQE value of **TTM-1DCz** significantly increased from 53.0 to 78.4%, and its k_{nr} decreased from 19×10^6 to $5 \times 10^6\text{ s}^{-1}$. The KIE of deuteration also made the luminescent radicals more stable, including redox stability, thermal stability, and photostability. Especially compared with non-deuterated radicals, the photostability of **TTM-2DCz** increased almost 10 times. These results from this paper demonstrate that the deuteration of relevant C-H bonds would

be an effective pathway to develop high-performance luminescent radicals, especially to the non-deuterated luminescent radicals with balanced k_{nr} and k_r . The influence of deuteration on the properties of radical-based light-emitting diodes are also under investigation.

Supplementary Materials: The following supporting information can be downloaded at: <https://www.mdpi.com/article/10.3390/molecules28124805/s1>, Figure S1: The synthetic routes of deuterated radicals. Figure S2: Mass spectrometry of deuterated radicals. Figure S3: Infrared absorption (IR) spectrogram of deuterated radicals. Figure S4: EPR of deuterated radicals in cyclohexane solution at room temperature. Figure S5: UV-Vis absorption spectra of deuterated radicals in solutions of different polarities (10–5 M). Figure S6: Transient fluorescence decay of deuterated radicals in cyclohexane solution (10–5 M). Figure S7: Voltammetry (CV) curves of non-deuterated radicals. Figure S8: Voltammetry (CV) curves of deuterated radicals for multiple (20-turn) cycles. Figure S9: TGA curve of deuterated radicals and non-deuterated radicals. Figure S10: Photostability of deuterated radicals and non-deuterated radicals. Table S1: Redox potentials and corresponding orbital energy levels of deuterated radicals and non-deuterated radicals. Table S2: The corresponding SOMO orbital energy levels calculated theoretically and measured experimentally. Table S3: Parameters corresponding to the emission bands in TD-DFT calculations of deuterated radicals.

Author Contributions: Methodology, formal analysis, investigation, data curation, writing—original draft, writing—review and editing, visualization, Z.M., L.Z. and Z.C.; conceptualization, investigation, validation, writing—review and editing, visualization, supervision, project administration, X.A. All authors have read and agreed to the published version of the manuscript.

Funding: This research was funded by the National Natural Science Foundation of China (No. 22105054), the Hainan Provincial Natural Science Foundation of China (Nos. 221RC1019, 222QN221), the Collaborative Innovation Center Foundation of Hainan University (No. XTCX2022XXC02), and the Hainan University Start-up Fund.

Institutional Review Board Statement: Not applicable.

Informed Consent Statement: Not applicable.

Data Availability Statement: The data presented in this study are available on request from the corresponding author.

Acknowledgments: Z.M., L.Z. and X.A. are grateful for the financial support from the National Natural Science Foundation of China (No. 22105054), the Hainan Provincial Natural Science Foundation of China (Nos. 221RC1019, 222QN221), the Collaborative Innovation Center Foundation of Hainan University (No. XTCX2022XXC02), and the Hainan University Start-up Fund. The authors are thankful for the support from the Analytical and Testing Center of Hainan University.

Conflicts of Interest: The authors declare no conflict of interest.

References

1. Ai, X.; Evans, E.W.; Dong, S.; Gillett, A.J.; Guo, H.; Chen, Y.; Hele, T.J.; Friend, R.H.; Li, F. Efficient radical-based light-emitting diodes with doublet emission. *Nature* **2018**, *563*, 536–540. [[CrossRef](#)] [[PubMed](#)]
2. Joo, Y.; Agarkar, V.; Sung, S.H.; Savoie, B.M.; Boudouris, B.W. A nonconjugated radical polymer glass with high electrical conductivity. *Science* **2018**, *359*, 1391–1395. [[CrossRef](#)] [[PubMed](#)]
3. Cui, Z.; Abdurahman, A.; Ai, X.; Li, F. Stable luminescent radicals and radical-based LEDs with doublet emission. *CCS Chem.* **2020**, *2*, 1129–1145. [[CrossRef](#)]
4. Obolda, A.; Zhang, M.; Li, F. Evolution of emission manners of organic light-emitting diodes: From emission of singlet exciton to emission of doublet exciton. *Chin. Chem. Lett.* **2016**, *27*, 1345–1349. [[CrossRef](#)]
5. Ma, T.; Li, C.-H.; Thakur, R.M.; Tabor, D.P.; Lutkenhaus, J.L. The role of the electrolyte in non-conjugated radical polymers for metal-free aqueous energy storage electrodes. *Nat. Mater.* **2023**, *22*, 495–502. [[CrossRef](#)] [[PubMed](#)]
6. Mao, L.; Zhou, M.; Shi, X.; Yang, H.-B. Triphenylamine (TPA) radical cations and related macrocycles. *Chin. Chem. Lett.* **2021**, *32*, 3331–3341. [[CrossRef](#)]
7. Li, X.; Tan, W.; Bai, X.; Li, F. Stable Near-infrared-emitting Radical Nanoparticles for Fluorescence Imaging. *Chem. Res. Chin. U* **2023**, *39*, 192–196. [[CrossRef](#)]
8. Luo, J.; Rong, X.-F.; Ye, Y.-Y.; Li, W.-Z.; Wang, X.-Q.; Wang, W. Research progress on triarylmethyl radical-based high-efficiency OLED. *Molecules* **2022**, *27*, 1632. [[CrossRef](#)]

9. Kubo, T. Synthesis, physical properties, and reactivity of stable, π -conjugated, carbon-centered radicals. *Molecules* **2019**, *24*, 665. [[CrossRef](#)]
10. Wang, Z.; Zou, X.; Xie, Y.; Zhang, H.; Hu, L.; Chan, C.C.; Zhang, R.; Guo, J.; Kwok, R.T.; Lam, J.W. A nonconjugated radical polymer with stable red luminescence in the solid state. *Mater. Horiz.* **2022**, *9*, 2564–2571. [[CrossRef](#)]
11. Peng, Q.; Obolda, A.; Zhang, M.; Li, F. Organic light-emitting diodes using a neutral π radical as emitter: The emission from a doublet. *Angew. Chem. Int. Ed.* **2015**, *127*, 7197–7201. [[CrossRef](#)]
12. Obolda, A.; Ai, X.; Zhang, M.; Li, F. Up to 100% formation ratio of doublet exciton in deep-red organic light-emitting diodes based on neutral π -radical. *ACS Appl. Mater. Interfaces* **2016**, *8*, 35472–35478. [[CrossRef](#)] [[PubMed](#)]
13. Guo, H.; Peng, Q.; Chen, X.-K.; Gu, Q.; Dong, S.; Evans, E.W.; Gillett, A.J.; Ai, X.; Zhang, M.; Credgington, D. High stability and luminescence efficiency in donor–acceptor neutral radicals not following the Aufbau principle. *Nat. Mater.* **2019**, *18*, 977–984. [[CrossRef](#)] [[PubMed](#)]
14. Abdurahman, A.; Hele, T.J.; Gu, Q.; Zhang, J.; Peng, Q.; Zhang, M.; Friend, R.H.; Li, F.; Evans, E.W. Understanding the luminescent nature of organic radicals for efficient doublet emitters and pure-red light-emitting diodes. *Nat. Mater.* **2020**, *19*, 1224–1229. [[CrossRef](#)] [[PubMed](#)]
15. Mattiello, S.; Hattori, Y.; Kitajima, R.; Matsuoka, R.; Kusamoto, T.; Uchida, K.; Beverina, L. Enhancement of fluorescence and photostability of luminescent radicals by quadruple addition of phenyl groups. *J. Mater. Chem. C* **2022**, *10*, 15028–15034. [[CrossRef](#)]
16. Matsuda, K.; Xiaotian, R.; Nakamura, K.; Furukori, M.; Hosokai, T.; Anraku, K.; Nakao, K.; Albrecht, K. Photostability of luminescent tris (2, 4, 6-trichlorophenyl) methyl radical enhanced by terminal modification of carbazole donor. *Chem. Commun.* **2022**, *58*, 13443–13446. [[CrossRef](#)]
17. Hattori, Y.; Kitajima, R.; Ota, W.; Matsuoka, R.; Kusamoto, T.; Sato, T.; Uchida, K. The simplest structure of a stable radical showing high fluorescence efficiency in solution: Benzene donors with triarylmethyl radicals. *Chem. Sci.* **2022**, *13*, 13418–13425. [[CrossRef](#)]
18. Hattori, Y.; Tsubaki, S.; Matsuoka, R.; Kusamoto, T.; Nishihara, H.; Uchida, K. Expansion of Photostable Luminescent Radicals by Meta-Substitution. *Chem. Asian J.* **2021**, *16*, 2538–2544. [[CrossRef](#)]
19. Wu, C.; Ai, X.; Chen, Y.; Cui, Z.; Li, F. Effects of Introducing Halogen Atoms to Biphenylmethyl Radical on Photostability, Photophysical and Electroluminescent Properties. *Chem. J. Chin. U* **2020**, *41*, 972–980. [[CrossRef](#)]
20. Ding, J.; Dong, S.; Zhang, M.; Li, F. Efficient pure near-infrared organic light-emitting diodes based on tris (2,4,6-trichlorophenyl) methyl radical derivatives. *J. Mater. Chem. C* **2022**, *10*, 14116–14121. [[CrossRef](#)]
21. Dong, S.; Xu, W.; Guo, H.; Yan, W.; Zhang, M.; Li, F. Effects of substituents on luminescent efficiency of stable triaryl methyl radicals. *Phys. Chem. Chem. Phys.* **2018**, *20*, 18657–18662. [[CrossRef](#)] [[PubMed](#)]
22. Gao, Y.; Xu, W.; Ma, H.; Obolda, A.; Yan, W.; Dong, S.; Zhang, M.; Li, F. Novel luminescent benzimidazole-substituent tris (2,4,6-trichlorophenyl) methyl radicals: Photophysics, stability, and highly efficient red-orange electroluminescence. *Chem. Mater.* **2017**, *29*, 6733–6739. [[CrossRef](#)]
23. Tong, C.C.; Hwang, K.C. Enhancement of OLED efficiencies and high-voltage stabilities of light-emitting materials by deuteration. *J. Phys. Chem. C* **2007**, *111*, 3490–3494. [[CrossRef](#)]
24. Yao, J.; Dong, S.-C.; Tam, B.S.T.; Tang, C.W. Lifetime Enhancement and Degradation Study of Blue OLEDs Using Deuterated Materials. *ACS Appl. Mater. Interfaces* **2023**, *15*, 7255–7262. [[CrossRef](#)] [[PubMed](#)]
25. Peng, X.; Yeh, C.H.; Wang, S.F.; Yan, J.; Gan, S.; Su, S.J.; Zhou, X.; Zhang, Y.X.; Chi, Y. Near-Infrared OLEDs Based on Functional Pyrazinyl Azolate Os (II) Phosphors and Deuteration. *Adv. Opt. Mater.* **2022**, *10*, 2201291. [[CrossRef](#)]
26. Li, W.; Wu, A.; Fu, T.; Gao, X.; Wang, Y.; Xu, D.; Zhang, C.; Sun, Z.; Lu, Y.; Young, D.J. Improved efficiency and stability of red phosphorescent organic light-emitting diodes via selective deuteration. *J. Phys. Chem. Lett.* **2022**, *13*, 1494–1499. [[CrossRef](#)]
27. Cheng, J.-F.; Kong, F.-C.; Zhang, K.; Cai, J.-H.; Zhao, Y.; Wang, C.-K.; Fan, J.; Liao, L.-S. Positive isotope effect in thermally activated delayed fluorescence emitters based on deuterium-substituted donor units. *Chem. Eng. J.* **2022**, *430*, 132822. [[CrossRef](#)]
28. Murphy, R.B.; Staton, J.; Rawal, A.; Darwish, T.A. The Effect of Deuteration on the Keto–enol Equilibrium and Photostability of the Sunscreen agent Avobenzone. *Photochem. Photobiol. Sci.* **2020**, *19*, 1410–1422. [[CrossRef](#)]
29. Cai, Z.; Yan, W.; Guo, R.; Liu, H.; Huo, P.; Yu, G.; Bian, Z.; Liu, Z. Warm-White-Light Perdeuterated Dy (III) Complex with a Photoluminescence Quantum Yield of up to 72% in Deuterated Chloroform. *Inorg. Chem.* **2023**, *62*, 6560–6564. [[CrossRef](#)]
30. Velasco, D.; Castellanos, S.; López, M.; López-Calahorra, F.; Brillas, E.; Juliá, L. Red Organic Light-Emitting Radical Adducts of Carbazole and Tris(2,4,6-trichlorotriphenyl)methyl Radical That Exhibit High Thermal Stability and Electrochemical Amphotericity. *J. Org. Chem.* **2007**, *72*, 7523–7532. [[CrossRef](#)]
31. Ai, X.; Chen, Y.; Feng, Y.; Li, F. A Stable Room-Temperature Luminescent Biphenylmethyl Radical. *Angew. Chem. Int. Ed.* **2018**, *57*, 2869–2873. [[CrossRef](#)] [[PubMed](#)]
32. Frisch, M.J.; Trucks, G.W.; Schlegel, H.B.; Scuseria, G.E.; Robb, M.A.; Cheeseman, J.R.; Scalmani, G.; Barone, V.; Petersson, G.A.; Nakatsuji, H.; et al. (Eds.) *Gaussian 16*; Revision C.02; Gaussian, Inc.: Wallingford, CT, USA, 2019.

Disclaimer/Publisher’s Note: The statements, opinions and data contained in all publications are solely those of the individual author(s) and contributor(s) and not of MDPI and/or the editor(s). MDPI and/or the editor(s) disclaim responsibility for any injury to people or property resulting from any ideas, methods, instructions or products referred to in the content.